

Wound Healing in a Porcine Model of Retinal Holes

Madeline Evers Olufsen,¹ Jens Hannibal,^{2,3} Nina Buus Sørensen,¹
Anders Tolstrup Christiansen,¹ Ulrik Christensen,¹ Grazia Pertile,⁴
David H. Steel,⁵ Steffen Heegaard,^{1,6} and Jens Folke Kiilgaard^{1,2}

¹Department of Ophthalmology, Rigshospitalet, University of Copenhagen, Copenhagen, Denmark

²Faculty of Health and Medical Sciences, Institute of Clinical Medicine, University of Copenhagen, Copenhagen, Denmark

³Department of Clinical Biochemistry, Faculty of Health Sciences, Bispebjerg and Frederiksberg Hospital, University of Copenhagen, Copenhagen, Denmark

⁴IRCCS Sacro Cuore Don Calabria Hospital, Verona, Italy

⁵Bioscience Institute, Newcastle University, Newcastle Upon Tyne, United Kingdom

⁶Department of Pathology, Rigshospitalet, University of Copenhagen, Copenhagen, Denmark

Correspondence: Jens Folke Kiilgaard, Department of Ophthalmology, Section 7066, Rigshospitalet, Inge Lehmanns Vej 8, Copenhagen 2100, Denmark; jens.folke.kiilgaard@regionh.dk.

Received: April 17, 2024

Accepted: July 17, 2024

Published: August 26, 2024

Citation: Olufsen ME, Hannibal J, Sørensen NB, et al. Wound healing in a porcine model of retinal holes. *Invest Ophthalmol Vis Sci*. 2024;65(10):35. <https://doi.org/10.1167/iovs.65.10.35>

PURPOSE. To investigate retinal wound healing, we created a new porcine model of retinal hole and identified the cells involved in hole closure.

METHODS. Sixteen landrace pigs underwent vitrectomy, and a subretinal bleb was created before cutting a retinal hole using a 23G vitrector. No tamponade was used. Before surgery and one, two, and four weeks after surgery, the eyes were examined by optical coherence tomography and color fundus photos. At the end of follow-up, the eyes were enucleated for histology. Tissue sections of 5 μ m were prepared for hematoxylin-eosin staining and immunohistochemical analysis with antibodies to retinal glial and epithelial cells.

RESULTS. Retinal holes below 1380 μ m in diameter closed spontaneously within four weeks, whereas larger holes remained open. Hole closure was mediated by central movement of the edges of the hole and in most cases the formation of a gliotic plug. Fluorescence microscopy revealed that the plug consisted of cells positive for glial fibrillary acidic protein, indicating the presence of macroglial cell types. Specifically, the plug was positive for S100 calcium-binding protein B, mainly representing astrocytes, while it was negative for anti-glutamine synthetase, representing Müller glia. These findings suggest that astrocytes are the predominating cell type in the plug. Minimal glial reaction was seen in the retinal holes that did not close.

CONCLUSIONS. We present a new porcine model for investigating large retinal holes. The retinal holes closed by approximation of hole edges, and the remnant retinal defect was closed with an astroglial plug.

Keywords: healing process, pig, macular hole, immunohistochemistry, subretinal surgery

A macular hole (MH) is a full-thickness anatomic defect in the foveal neurosensory retina that causes severe visual impairment. The condition is predominately idiopathic (85%), with a smaller fraction attributed to causes such as trauma, inflammation, or high myopia.^{1,2} Although some MHs close spontaneously,^{3,4} the majority of MHs necessitate vitreoretinal surgery to achieve hole closure. The mechanism behind MH closure is not very well described. Theoretically, the relief of tangential traction applied to the MH after either vitrectomy or spontaneous posterior vitreous detachment results in reapproximation of the hole edges.^{5,6} Subsequently a wound-healing process commences. This has previously been attributed to a healing response mediated by the proliferation of retinal pigment epithelium (RPE) cells and glial cells.⁷ The formed tissue creates a bridge or plug to connect the hole edges. However, for large MHs refractory to initial surgery, the plugging might be harder or the

healing response may not be adequately stimulated because they more often fail to close.⁸

Three histopathological studies on eyes with closed MHs after vitreoretinal surgery have been reported.^{9–11} In most cases, a remnant retinal defect, much smaller than the preoperative hole diameter, was observed in the closed MHs. Transmission electron microscopy revealed that the tissue consisted of cells with feature characteristics of either Müller glia^{10,11} or fibrous astrocytes.⁹ Similar observations were found in studies of spontaneously closed MHs.^{12,13} Nonetheless, consensus on the predominant cell type involved in hole closure has not been reached.

In this experimental study, we investigated the dynamic process of retinal hole closure in a porcine model. The porcine eye has no macula or fovea but a horizontal band, known as the “visual streak,” characterized by a high density of ganglion cells and photoreceptors akin to the human

parafoveal macula.^{14,15} Additionally, the porcine eye closely resembles the human eye in terms of size and vascularization.¹⁶ We hypothesized that a retinal hole in the visual streak undergoes a closure process similar to that observed in MH in humans. If the retinal hole is very large, closure may not occur, yet the dimensional limit for this outcome remains unknown. With this *in vivo* porcine study, we aimed to examine the natural course of retinal holes across a range of sizes, utilizing optical coherence tomography (OCT) and comprehensive histopathological analyses.

METHODS

Left eyes from 16 immunocompetent Danish Landrace pigs underwent surgery. Thirteen eyes were included in the study because three pigs were euthanized at the time of the primary surgery because of other illnesses unrelated to the eye. One eye with a large retinal hole, measuring 1900 μm , was excluded from further analysis because an extensive retinal detachment made it impossible to measure hole size at follow-up examinations, and histological preparation was not performed. At baseline, the pigs were three months old and weighed approximately 25 kg. All animal treatment was supervised by a veterinarian and was in accordance with the ARVO statement on the use of animals in ophthalmic and vision research. The research protocol was approved by the Danish Animal Experiment Committee (no. 2019-15-0201-01652).

Surgical Procedure and Follow-Up Regimen

After disinfection (5% povidone iodine, SAD) a 360° peritomy was performed, and three sclerotomies were made, 1 mm posterior to the corneal limbus, and 23-gauge trocars were inserted. An infusion line with balanced saline solution (PLUS Irrigating Solution; Alcon, Geneva, Switzerland) was attached to one of the trocars. The pigs underwent standard core vitrectomy including induction of a posterior vitreous detachment using a 23G vitrectomy probe (Constellation, 23GA totalplu, 7500 CPM Ultravit Probe; Alcon). To detach the neuroretina from the underlying RPE, a subretinal bleb was created by injecting balanced saline solution into the subretinal space through a 38G cannula (38-gauge/0.12 mm, PolyTip, MedOne) using the MedOne microdose injector system (MicroDose Injector; MedOne Surgical Inc., Sarasota, FL, USA) at a maximum pressure setting of 28 PSI on the vitrectomy machine (Constellation; Alcon). Subsequently, a retinal hole of different size was then created using the vitrectomy probe. The hole was located within the temporal visual streak at approximately the same distance from the optic nerve. To obtain different hole sizes, we used a combination of preoperative OCT scan measurements of landmarks (e.g., optic nerve diameter, vessel diameter, and distance between vessels) and the perioperative use of a FINNESSE Flex loop (25G; Alcon Grieshaber, Schaffhausen, Switzerland) as a measurement tool. Retinal bleeding was only coagulated with diathermy if required. Internal limiting membrane (ILM) peeling was not performed, and no tamponade was used. Sclera and conjunctiva were sutured with Vicryl 7-0 (Ethicon, Bridgewater, NJ, USA), and at the end of the procedure, chloramphenicol ointment (Kloramfenikol "DAK"; Nycomed, Roskilde, Denmark) was applied.

All 13 eyes were examined before and immediately after surgery with color fundus photography (CFP) and OCT

(Spectralis, Heidelberg, Germany) modified to examine the anesthetized pig. Imaging was repeated at follow-up examinations at one, two, and four weeks after surgery, using the follow-up function on Heidelberg OCT. The baseline scan immediately after surgery served as the reference scan for the subsequent scans. This minimized the error of measurements between examinations. The B-scan representing the largest diameter of the hole was used to measure the distance between the outer nuclear layers (ONL) on both sides of the hole. This method may have overestimated the largest basal diameter in comparison with the situation, where the retina was in contact with the RPE, but we estimate that the error was similar in all cases, and we did not try to compensate for this error. In case the hole was closed and the central part had lost retinal lamination, the distance between preserved retinal layering was measured at the ONL level. This distance was classified as a "retinal plug."

Anesthesia

All surgeries and follow-up examinations were performed with the animals under full anesthesia. The pigs were preanesthetized, and the pupil was dilated with a topical combination of 0.4% benoxinate hydrochloride (Oxybuprocaine; SAD, Copenhagen, Denmark), 10% phenylephrine hydrochloride (Metaoxedrinechloride; SAD), 0.5% tropicamide (Mydriacyl; Alcon), and 1% atropine sulfate (SAD). Next the pigs were endotracheally intubated and anesthetized by inhalation of 3.0% isoflurane (isoflurane [USP]; Abbott Laboratories, Abbott Park, IL, USA) and fentanyl (Fentanyl "hameln"; Matrix Pharmaceuticals, Hellerup, Denmark). During the procedure they were artificially ventilated. At the end of the follow-up period the pigs were euthanized with 1 mL/kg pentobarbital 200 mg/mL lidocaine hydrochloride 20 mg/mL intravenously (Glostrup Pharmacy, Glostrup, Denmark), and the eyes were enucleated.

Histological Preparation and Staining

Twelve eyes were examined histologically at either one week ($n = 3$), two weeks ($n = 1$), or four weeks ($n = 8$). The enucleated eyes were immediately fixed in 4% paraformaldehyde. Segments containing the optic disc and the area with the retinal hole were cut out and embedded in paraffin. Five sections of 5 μm were cut every 50 μm through the lesion, and every fifth section underwent hematoxylin and eosin staining. The sections were examined in a light microscope (Axioplan 2; Carl Zeiss, Inc., White Plains, NY, USA), and digital images were acquired using an Axiocam (Axiocam 208 color, Carl Zeiss, Germany) and Zen (Zen blue 3.5; Carl Zeiss Microscope GmbH, Jena, Germany). Unstained sections containing the retinal hole were selected for immunohistochemical (IHC) analysis. After deparaffinization, the sections underwent antigen retrieval at pH 6 (EnvisionFLEX, Target Retrieval Solution, LowpH, no. GV805; Dako Omnis, Agilent Technologies, Winooski, VT, USA) in an oven set at 80° C for 1.5 hours. Primary antibodies for identification of retinal cells are specified in the Table. Anti-GFAP were used to detect macroglia, anti-S100B mainly to detect astrocytes and anti-GS to detect Müller glia and.^{17,18} Anti-CK-AECAM was used as an epithelial marker to identify RPE cells. Primary antibodies for inner retinal neurons included anti-PKC α for rod bipolar cells^{19,20} and anti-TH for dopamine containing amacrine cells.^{19,21} All primary antibodies were incubated with the specimen

TABLE. Primary Antibodies

Primary Antibody	Host	Source	Dilution	Müller Glia	Astrocytes	RPE Cells	Amacrine Cells	Bipolar Cells	Plug
GFAP	Rabbit	Dako no. Z033429-2	1:2000	+	+	-	-	-	+
S100B	Mouse	Sigma-Aldrich no. S2532	1:500	-	+	-	-	-	+
GS	Rabbit	Sigma-Aldrich no. G2781	1:1000	+	-	-	-	-	-
CK-AECAM	Mouse Rabbit	Agilent no. IR053 no. IR094	1:1	-	-	+	-	-	-
PKC α	Mouse	Sigma-Aldrich no. P5704	1:500	-	-	-	-	+	-
TH	Rabbit	Chemicon no. AB152	1:500	-	-	-	+	-	-

Primary antibodies used to identify Müller glia, astrocytes, neuroepithelial cells (RPE), amacrine cells, and bipolar cells in the porcine retina. Positive and negative staining of the cells is shown with “+” and “-.” Markers found in the retinal plug are seen in the column on the far right.

overnight, whereas secondary antibodies were incubated for two hours. Sections were mounted with glycerol/water (1:1) and DAPI (1:1000). Fluorescence micrographs were obtained using an iMIC confocal microscope (Till Photonics, FEI, Munich, Germany).¹⁹

Data Analysis

Repeated measurements of the retinal defect at the follow-up examinations for each eye were analyzed in R (R version 4.1.3). The difference between the mean hole size of closed and open retinal holes was analyzed using a Mann-Whitney test. P values < 0.05 were considered significant. All histology was thoroughly examined by one assessor, and the areas of interest were evaluated and discussed within the research group.

RESULTS

Baseline retinal hole measurements were available in 11 out of 12 eyes with postoperative OCT, because imaging from one eye was lost because of technical problems. Retinal hole

sizes were re-measured on OCT scans after one week in two eyes, after two weeks in five eyes, and after four weeks in eight eyes. After four weeks of follow-up, six retinal holes were closed, and three remained open (Fig. 1A). In one of the eyes where the hole closed, a peripheral retinal detachment (RD) was observed after two weeks. This resolved after four weeks but resulted in a retinal fold, and we excluded this from further hole size analysis (Fig. 1A). Retinal hemorrhage within the retinal hole was observed on postoperative OCT scans in six eyes, one of which was treated with diathermy during surgery. Iatrogenic cataract was observed peripherally in one eye in relation to a trocar. Choroidal neovascularization was seen both on OCT and histologically in two eyes in relation to the area, where the subretinal bleb was initiated. No cystoid changes were observed during follow-up.

OCT Findings

There was a significant difference (Wilcoxon, $P = 0.036$) in baseline hole size between retinal holes that remained open (mean = 1562 μm) or had closed (mean = 1130 μm)

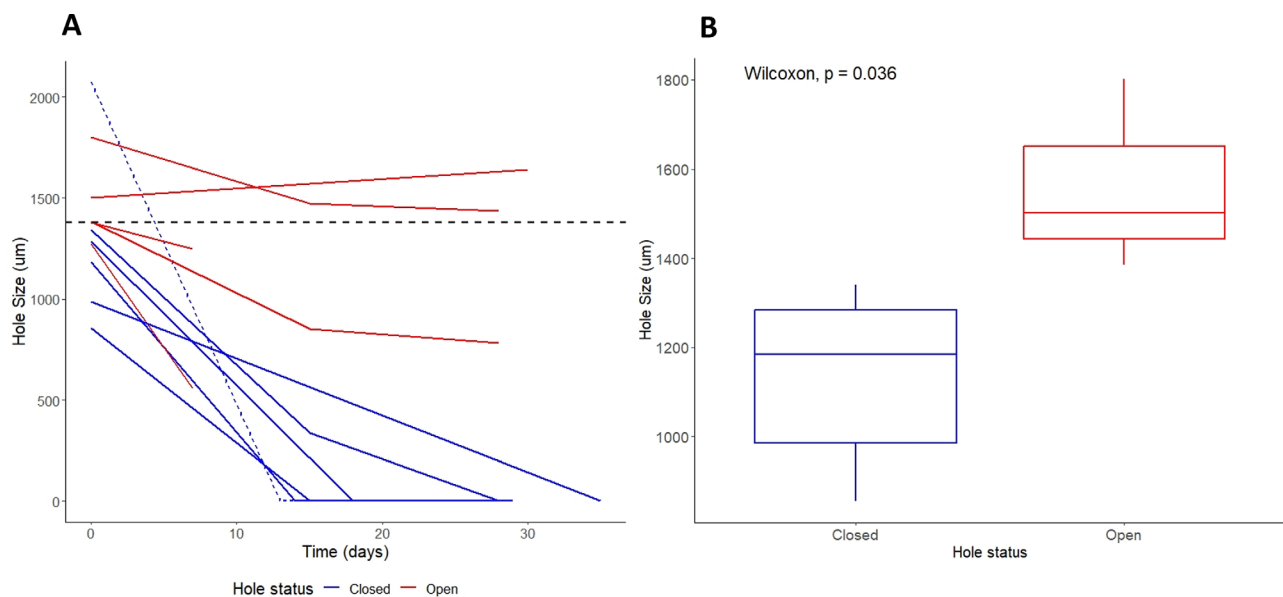


FIGURE 1. Hole size during follow-up. (A) Hole size measurements just after surgery and at follow-up examinations. The horizontal stippled line at 1380 μm represents the approximate threshold for spontaneous hole closure. The largest hole in the study (2073 μm) exhibited a retinal fold and was excluded from further hole size analysis (stippled blue line). Blue lines illustrate closed holes. Red lines illustrate open holes. (B) Mean basal hole size of closed (1130 μm) and open (1562 μm) retinal holes at four weeks were significantly different ($P = 0.036$). The boxplot illustrates the size of the holes of the closed ($n = 5$) versus open ($n = 3$) retinal holes (median, IQR, absolute range).

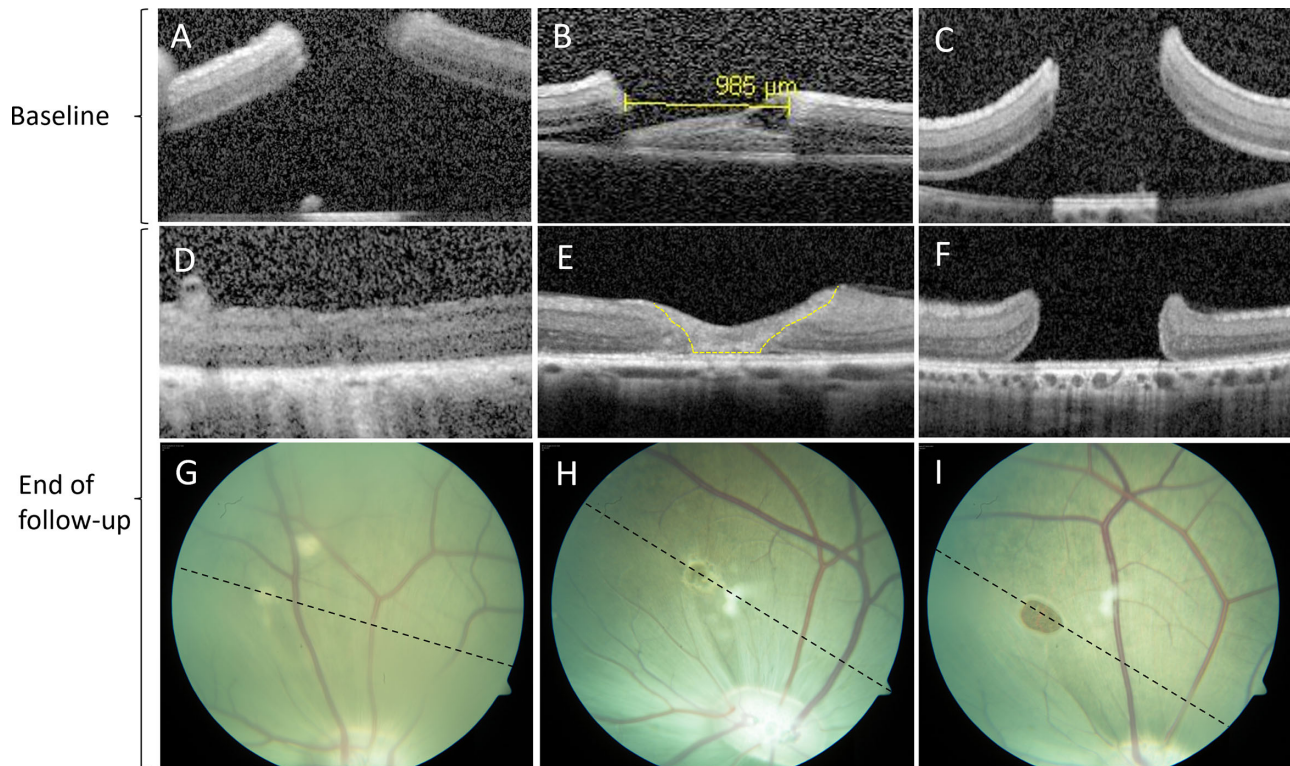


FIGURE 2. Optical coherence tomography and color fundus photography at baseline and at the end of follow-up. Just after surgery (baseline) the edges of the hole were elevated from the RPE, and the retinal layers were preserved (A–C). Retinal holes below 1380 μm at baseline closed spontaneously, either with complete apposition of the retinal hole margins (D) or with a gliotic structure, classified as a retinal plug (E, *yellow dotted line*). Retinal holes above 1380 μm at baseline remained open at the end of follow-up (I), and the retinal layers appeared intact at the hole margins (F). The *stippled black line* on CFP illustrates the direction of the final OCT scan (G–I). The closed holes appeared hypopigmented on CFP (G, H).

after four weeks (Fig. 1B). The boxplot in Figure 1B illustrates the basal hole size of the two groups. For the closed holes ($n = 5$) the median was 1184 μm (range 854–1341 μm) with an interquartile range (IQR) of 299 μm . For the

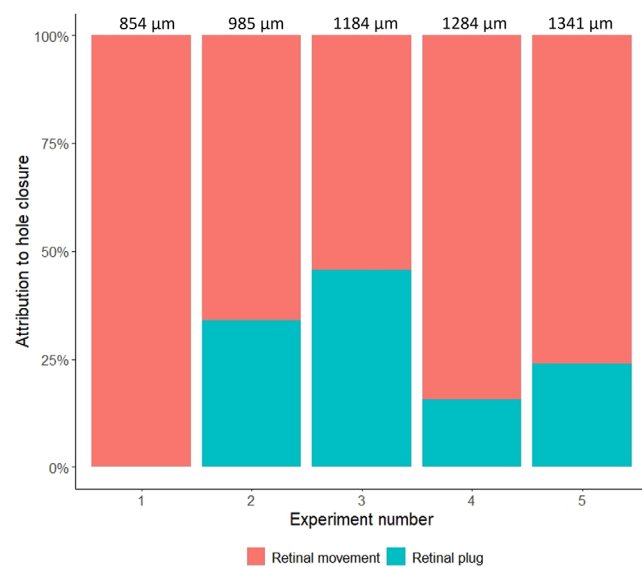


FIGURE 3. Closure mechanism of retinal holes. The bars represent attribution of the retinal plug (*blue*) and the movement of the retinal hole borders (*red*) compared to the baseline hole size for each closed retinal hole (smallest to largest basal hole diameter).

open holes ($n = 3$) the median was 1502 μm (1384–1801 μm) with an IQR of 208 μm . The cutoff baseline hole size for spontaneous closure was estimated to be above 1380 μm , representing the diameter of the smallest hole that did not close (Fig. 1A). The slope of the hole size differed between closed and open holes. Holes that achieved closure tended to exhibit a steeper slope compared to those that remained open after four weeks. In the two eyes with one-week follow-up, it is likely that the smaller hole would have closed spontaneously, although the larger hole might have remained open (Fig. 1A).

Just after surgery the edges of the hole were elevated from the RPE, but the retinal layers were preserved (Figs. 2A–C). In one of the cases where the retinal hole closed, the hole edges re-apposed completely (Fig. 2D). In the remaining five cases the central part of the retinal hole was seen as a gliotic structure on OCT (Fig. 2E). This amorphous structure, classified as a retinal plug, was in all cases smaller than the baseline diameter of the retinal hole. Figure 3 shows the attribution of the retinal plug and the movement of the borders of the retinal hole compared to the baseline hole diameter. In the open retinal holes, the retinal layering appeared intact at the hole margins (Fig. 2F). On the fundus images the closed holes appeared hypopigmented (Figs. 2G–H).

Histology Findings

Twelve eyes underwent histological examination. Three eyes were enucleated after one week, one eye after two weeks,

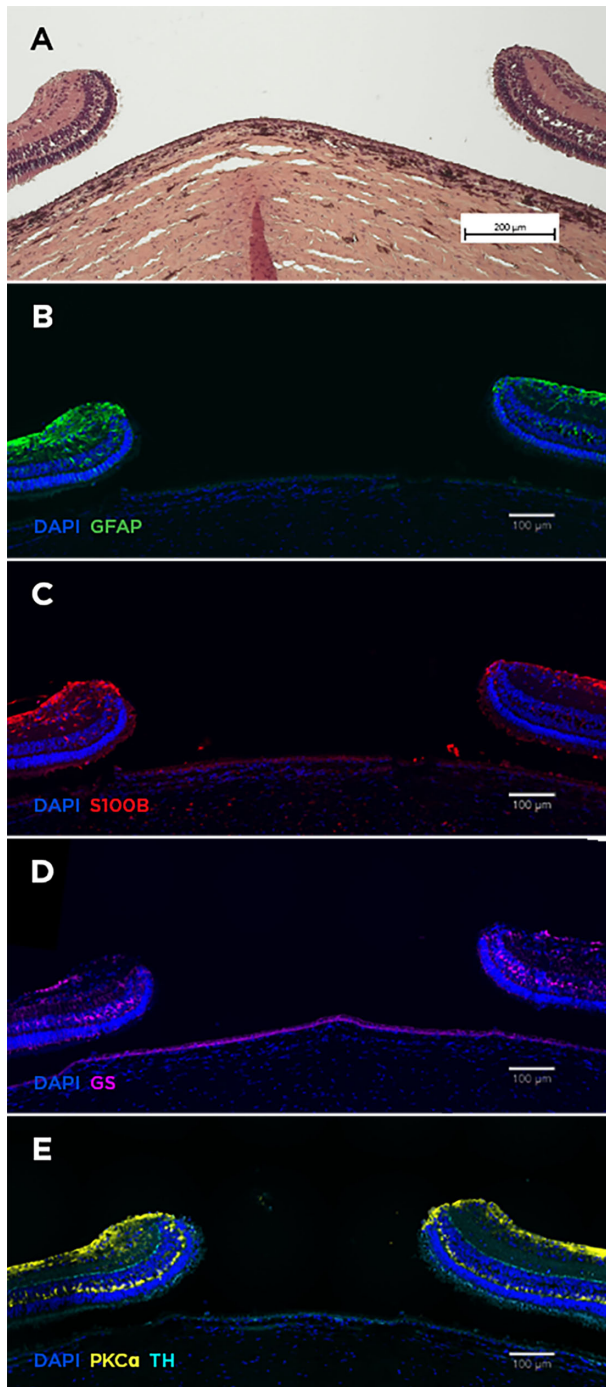


FIGURE 4. Histology of open retinal holes. Hematoxylin and eosin staining showed inert retina at the hole edges (A). Minimal glial reaction (anti-GFAP, anti-S100B, anti-GS) was observed (B–D). Markers for bipolar (anti-PKC α) and amacrine cells (anti-TH) confirmed preservation of retinal layering at the hole margins (E).

and eight eyes four weeks after surgery. Minimal glial reaction was seen in the open retinal holes, despite single astrocytic cells extending to the INL near the hole margins (Figs. 4A–D). The application of anti-TH and anti-PKC α confirmed the preservation of retinal structure and revealed the presence of amacrine cells and bipolar cells extending to the hole margins (Fig. 4E). Scattered lymphocytes and fibroblasts were present in the choroid, but not in

the retina, after one and two weeks but not at four weeks (Fig. 5).

The Retinal Plug

Closed retinal holes were sealed with a retinal plug of variable dimensions. The plug disrupted the neuroretina, while the underlying RPE layer appeared normal (Fig. 5A). After one week we observed that the initial plug bridged the external retina on both sides of the hole (Fig. 5B). IHC analysis of the retinal plugs is presented in the Table. The retinal plugs stained positive for anti-GFAP, which indicated that they consisted of macroglial cells, more specifically Müller glia and astrocytes (Figs. 5C–D). To differentiate between Müller glia and astrocytes additional glial cell staining were conducted. We found positive anti-S100B staining throughout the plug (Figs. 5E–F), while anti-GS staining was negative in the plug (Fig. 5I). Untouched retina adjacent to the hole served as control. In these areas, Müller glia expressed both GFAP and GS throughout the retina. In contrast, S100B were merely confined to the nerve fiber layer and ganglion cell layer, corresponding to the location of astrocytes. Anti-CK-AECAM, representing RPE cells, stained negative in the plug (see Supplementary Fig. S1). When merging anti-GFAP and anti-S100B we found increased colocalization in the plug (Figs. 5G–H). These findings together suggest that astrocytes were the predominant cell type in the retinal plug. In 1 out of 6 eyes the retinal plug was absent, and the retinal layers had merged (Fig. 5J), as observed in the corresponding OCT scan (Fig. 2D), with minimal glial proliferation (Figs. 5K–M).

DISCUSSION

In this study, we show that iatrogenic retinal holes in the posterior pole of the porcine retina heal in a hole size dependent manner. Retinal holes below 1380 μ m in diameter closed spontaneously within four weeks, whereas larger holes remained open. Interestingly, the holes that remained open showed minimal signs of scar reaction and inflammation. Retinal hole closure was mediated by approximation of the edges of the hole and in most cases the formation of a retinal plug.

Analysis of the retinal plug demonstrated a process characterized by proliferation and migration of glial cells into the retinal hole. The retinal glial cell population includes Müller glia, astrocytes, and microglia.²² Among these, Müller glia and astrocytes seem to be the most likely candidates involved in retinal repair. In the healthy retina, Müller glia are radial cells extending from the vitreous retinal border to the distal end of the ONL, while astrocytes are confined to the nerve fiber layer and ganglion cell layer.^{17,22} In the retinal plug, however, the structural retinal layering was disrupted, and the nuclei were scattered throughout the plug. This made it impossible to distinguish between the cell types based on structural characteristics and localization. IHC analysis of the retinal plug revealed a positive reaction for anti-GFAP, but as GFAP is expressed in both astrocytes and Müller glia in the distressed retina,¹⁷ this merely indicated the presence of macroglia cells. Interestingly, the retinal plug stained negative for anti-GS, which is exclusively found in Müller glia. There is a possibility that Müller glia may downregulate the expression of GS as earlier described in cases with reactive gliosis.²² No specific astrocytic marker in the retina

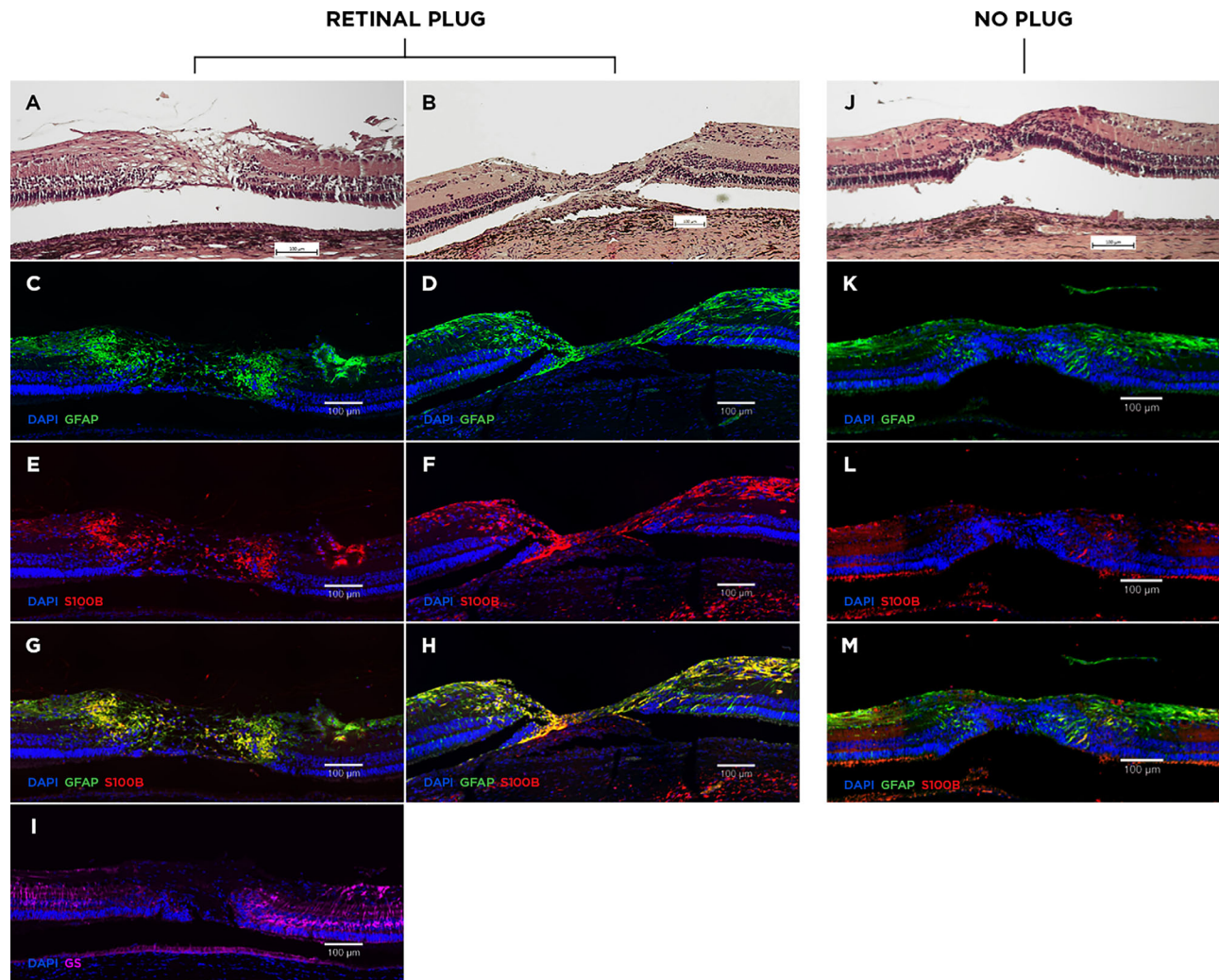


FIGURE 5. Histology of closed retinal holes. The majority of holes closed with a retinal plug within four weeks (**A**). Initial stages of a plug were observed after one week (**B**). The retinal plugs stained positive for anti-GFAP (**C**, **D**) and anti-S100B (**E**, **F**), and negative for anti-GS (**I**). Anti-GFAP stained both Müller glia and astrocytes, while the anti-S100B- and anti-GS-positive staining corresponded to astrocytes and Müller glia, respectively. Merging of anti-GFAP and anti-S100B showed increased co-localization in the retinal plug (**G**, **H**, yellow). In one case no plug was observed, and the retinal layers positioned each other (**J**). Minimal glial proliferation was observed at the merged hole margins (**K**–**M**). Scattered lymphocytes and fibroblasts were present in the choroid after one and two weeks but were not seen after four weeks (**B** + **J**).

has been described.²² S100B is a calcium-binding protein predominately found in astrocytes in the nervous system, but it has also been reported to be expressed by human retinal Müller glia.¹⁸ However, in our analysis, the location of S100B positive cells in the surrounding porcine retina, which served as our control, corresponded to that of astrocytes. This was further supported by the absence of colocalization, when anti-S100B and anti-GS were merged (see Supplementary Fig. S2). The positive anti-GFAP and anti-S100B staining of the plug, in conjunction with the negative anti-GS staining, led us to conclude that the retinal plugs predominately consisted of astrocytes.

These findings align with the previous histopathological investigations of post-mortem human eyes with closed MH. Consensus on whether the remnant retinal defect is predominantly composed of astrocytes, Müller glia or RPE cells, however, has not been reached. In a study of spontaneous closed macular holes, Guyer et al. reported that the holes closed due to fibroglial proliferation or RPE hyperplasia.

¹² Three histopathologic studies of eyes with successful hole closure after MH surgery (vitrectomy and gas tamponade) reported anatomical repair of the MHs with proliferation of either fibrous astrocytes⁹ or Müller glia.^{10,11} These findings were all established through identification of cellular structures and characteristics using light and transmission electron microscopy. Later, Yamana et al.²³ investigated retinal healing in a rabbit model of retinal holes measuring 500 µm using IHC. Hole closure was achieved in gas-injected eyes after one week, while holes without gas tamponade remained open after three months. In the closed holes both anti-GFAP and anti-Cytokeratin 18 positive cells, representing glial and RPE cells, were identified. However, they did not distinguish between the macroglial cell types. In our porcine model, much larger retinal holes closed without gas tamponade, and we did not find cytokeratin (anti-CK-AECAM) positive cells in the plug. Thus there may be a difference in the reparative process between species.

The retinal plug could only account for less than 50% of the hole closure. The central retinal movement of the borders of the hole cannot be solely explained by overestimating the hole size at baseline due to elevated edges of the hole. In the case, where no plug was observed, retinal stretching must have taken place as retinal tissue was removed in the production of the hole. As the major part of the hole closure was not attributed to the retinal plug, we postulate that retinal stretching must also have taken place in these cases. In the case with a closed retinal hole one week postoperatively, we observed that the initial stages of plug formation bridged the edges of the hole. This implies that the retinal plug may contribute to the centripetal retinal movement, possibly through contraction early in the process. This observation may also explain the difference in closure rates between the closed and open holes, as illustrated by the slopes of hole size over time (Fig. 1.), indicating a variation in the centripetal force between the two groups. These findings are consistent with previous histopathological studies of MH closed after vitreoretinal surgery.^{9–11} Most cases revealed a persisting retinal defect measured as the gap between the external limiting membrane, which was considerably smaller than the preoperative MH.^{9–11} In the studies by Madreperla et al.¹⁰ and Rosa et al.,¹¹ cases with a similar preoperative hole size (Stage III macular hole) showed a persisting defect of 16 μm and 250 μm , respectively. The variation might be attributed to the follow-up time between surgery and enucleation, because there were seven months of follow-up in the first case compared with two months in the second case. These observations reinforce the concept of gradual contraction of the retinal plug, which suggests that the surrounding retina is capable of stretching. The theory of retinal stretching as a major contributor to hole closure is further supported by the fact that ILM peeling in humans highly increases the chance of hole closure because removal of the ILM makes the retina more mobile.^{24,25}

In our study, glial cell proliferation seemed dependent on the basal retinal hole size. The smallest hole in our study, measuring 854 μm at baseline, closed with complete approximation of the edges of the hole. In the larger retinal holes, closure was accompanied by the proliferation and migration of glial cells to form the retinal plug. Interestingly, there was minimal glial reaction in the margins of the open retinal hole, suggesting that there is a maximal hole size above which the retinal healing response is inadequate. Histopathological findings by Funata et al.⁹ likewise described one case with apposed macular hole edges and no sign of glial proliferation. Studies examining OCT images of closed MHs also suggest an association between preoperative hole size, glial proliferation and visual recovery.^{26,27} Oh et al.²⁶ found a higher prevalence of glial proliferation in eyes with large preoperative basal diameters compared to those with small preoperative basal hole diameters, and these exhibited greater photoreceptor layer defects, resulting in poorer visual outcome. The precise cellular mechanisms responsible for inducing the glial cell proliferation remain unclear. Previous studies of retinal wound healing in rabbits suggested that macrophages present at the wound site appeared to be the major stimulus for cellular proliferation.²⁸ However, our observations suggest the distance between the hole margins may also have an impact. If the distance is excessively large, inducement of glial proliferation fails. To investigate whether a cell-to-cell communication exists, it would be valuable to compare

protein expressions at the margins of open holes to that of closed holes. In this way the effect of the trauma would be isolated. This would provide a comprehensive understanding of the cellular mechanisms involved in retinal healing.

The porcine model, presented in this study, seems to be useful in the investigation of large retinal holes. Despite the creation of large central holes, RD was only observed in two out of 13 eyes. These two cases represented the largest retinal holes in the study, measuring 1900 μm and 2073 μm , respectively. This suggests that porcine RPE cells of the posterior pole may possess the same ability as central human RPE cells, namely to pump out significant amounts of subretinal fluid.²⁹ However, there appears to be a saturation point. Nevertheless, it is noteworthy that central holes in the porcine retina can attain considerable dimensions without resulting in RD, just as MHs in humans. This feature makes the porcine retina an ideal animal model for investigating large retinal holes.

It is important to acknowledge the limitations of the model. Our porcine model does not have the same pathology as human MHs. Holes were formed by removal of retinal tissue rather than dehiscence and the trauma induced in their production, might have enhanced the glial cell proliferation response observed. However, as ILM peeling in standard MH surgery is also thought to trigger glial cell proliferation,^{25,30} we postulate that the postoperative retinal changes may be analogous. Retinal hemorrhage within the created retinal hole may also have promoted hole closure, as seen in patients with MH treated with an autologous blood clot.³¹ Another limitation is that the pigs included in our study were approximately three months old at the time of inclusion, making their retina comparable to that of a young child. Thus their healing response may be more active than that of the typical MH patient who is in their sixth or seventh decade.^{32,33} This may account for the spontaneous closure of very large holes in our model. For comparison, spontaneous closure of idiopathic MHs rarely occurs when the hole exceeds 400 μm .^{2,34} Furthermore, our findings are limited by a relatively short follow-up period. Consequently, we lack information about potential structural remodeling and further shrinkage of the retinal plug over time. Moreover, we remain uncertain about whether the open retinal holes would have closed over time, although the slopes in the plot depicting hole size over time (Fig. 1) suggest that hole closure would not have been achieved without further surgical intervention.

CONCLUSIONS

We present a porcine model for investigating retinal holes. Retinal holes below 1380 μm closed spontaneously, whereas larger holes remained open for at least four weeks. Retinal holes closed by approximation of edges of the hole and the remnant retinal defect was closed with an astroglial plug.

Acknowledgments

Disclosure: **M.E. Olufsen**, None; **J. Hannibal**, None; **N.B. Sørensen**, None; **A.T. Christiansen**, None; **U. Christensen**, None; **G. Pertile**, None; **D.H. Steel**, Alcon (C, R), Roche (C, R), Alimera (C), BVI (C, R), complement therapeutics (C), DORC (C, R), Eyepoint (C), Bayer (R), Boehringer (R), Gyroscope (R); **S. Heegaard**, None; **J.F. Kiilgaard**, Aura Biosciences (C)

References

- Ezra E. Idiopathic full thickness macular hole: natural history and pathogenesis. *Br J Ophthalmol*. 2001;85:102–108.
- la Cour M, Friis J. Macular holes: Classification, epidemiology, natural history and treatment. *Acta Ophthalmol Scand*. 2002;80:579–587.
- Tadayoni R, Massin P, Haouchine B, Cohen D, Erginay A, Gaudric A. Spontaneous resolution of small stage 3 and 4 full-thickness macular holes viewed by optical coherence tomography. *Retina*. 2001;21:186–189.
- Chew EY, Sperduto RD, Hiller R, et al. Clinical course of macular holes: the Eye Disease Case-Control Study. *Arch Ophthalmol*. 1999;117:242–246.
- Kang SW, Ahn K. Types of macular hole closure and their clinical implications. *Br J Ophthalmol*. 2003;87:1015–1019.
- Smiddy WE, Flynn HW. Pathogenesis of macular holes and therapeutic implications. *Am J Ophthalmol*. 2004;137:525–537.
- Gregor ZJ. Surgery for idiopathic full-thickness macular holes. *Eye*. 1996;10(Pt 6):685–690.
- Steel DH, Donachie PHJ, Aylward GW, et al. Factors affecting anatomical and visual outcome after macular hole surgery: findings from a large prospective UK cohort. *Eye*. 2021;35:316–325.
- Funata M, Wendel RT, De La Cruz ZA, Green WR. Clinicopathologic study of bilateral macular holes treated with pars plana vitrectomy and gas tamponade. *Retina*. 1992;12:289–298.
- Madreperla SA, Geiger GL, Funata M, de la Cruz Z, Green WR. Clinicopathologic correlation of a macular hole treated by cortical vitreous peeling and gas tamponade. *Ophthalmology*. 1994;101:682–686.
- Rosa J, Glaser BM, De la Cruz Z, Green WR. Clinicopathologic correlation of an untreated macular hole and a macular hole treated by vitrectomy, transforming growth factor- β_2 , and gas tamponade. *Am J Ophthalmol*. 1996;122:853–863.
- Guyer DR, Richard Green W, De Bustros S, Fine SL. Histopathologic Features of Idiopathic Macular Holes and Cysts. *Ophthalmology*. 1990;97:1045–1051.
- Frangieh GT, Green WR, Engel HM. A histopathologic study of macular cysts and holes. 1981. *Retina*. 2005;25(5 Suppl.):311–336.
- García M, Ruiz-Ederra J, Hernández-Barbáchano H, Vecino E. Topography of pig retinal ganglion cells. *J Comp Neurol*. 2005;486:361–372.
- Chandler MJ, Smith PJ, Samuelson DA, Mackay EO. Photoreceptor density of the domestic pig retina. 1999;2:179–184.
- Simoens P, De Schaepdrijver L, Lauwers H. Morphologic and clinical study of the retinal circulation in the miniature pig. A: morphology of the retinal microvasculature. *Exp Eye Res*. 1992;54:965–973.
- Reichenbach A, Bringmann A. Glia of the human retina. *Glia*. 2020;68:768–796.
- Michetti F, D'Ambrosi N, Toesca A, et al. The S100B story: from biomarker to active factor in neural injury. *J Neurochem*. 2019;148:168–187.
- Hannibal J, Christiansen AT, Heegaard S, Fahrenkrug J, Kiilgaard JF. Melanopsin expressing human retinal ganglion cells: Subtypes, distribution, and intraretinal connectivity. *J Comp Neurol*. 2017;525:1934–1961.
- Johansson UE, Eftekhari S, Warfvinge K. A battery of cell- and structure-specific markers for the adult porcine retina. *J Histochem Cytochem*. 2010;58:377–389.
- Christiansen AT, Folke J, Kristian K, Paul D, Woldbye D, Hannibal J. Localization, distribution, and connectivity of neuropeptide Y in the human and porcine retinas — A comparative study. *J Comp Neurol*. 2018;526:1877–1895.
- Vecino E, Rodriguez FD, Ruzafa N, Pereiro X, Sharma SC. Glia-neuron interactions in the mammalian retina. *Prog Retin Eye Res*. 2016;51:1–40.
- Yamana T, Kita M, Ozaki S, Negi A, Honda Y. The process of closure of experimental retinal holes in rabbit eyes. *Graefes Arch Clin Exp Ophthalmol*. 2000;238:81–87.
- Christensen UC. Value of internal limiting membrane peeling in surgery for idiopathic macular hole and the correlation between function and retinal morphology. *Acta Ophthalmol*. 2009;87(thesis2):1–23.
- Chatziralli IP, Theodosiadis PG, Steel DHW. Internal limiting membrane peeling in macular hole surgery; why, when, and how? *Retina*. 2018;38:870–882.
- Oh J, Yang SM, Choi YM, Kim SW, Huh K. Glial proliferation after vitrectomy for a macular hole: a spectral domain optical coherence tomography study. *Graefes Arch Clin Exp Ophthalmol*. 2013;251:477–484.
- Ko TH, Witkin AJ, Fujimoto JG, et al. Ultrahigh-resolution optical coherence tomography of surgically closed macular holes. *Arch Ophthalmol*. 2006;124:827–836.
- Miller B, Miller H, Patterson R, Ryan SJ. Retinal wound healing. Cellular activity at the vitreoretinal interface. *Arch Ophthalmol*. 1986;104:281–285.
- Marmor MF. Control of subretinal fluid: experimental and clinical studies. *Eye*. 1990;4(Pt 2):340–344.
- Madi HA, Masri I, Steel DH. Optimal management of idiopathic macular holes. *Clin Ophthalmol*. 2016;10:97–116.
- Zhu D, Ma B, Zhang J, et al. Autologous blood clot covering instead of gas tamponade for macular holes. *Retina*. 2020;40:1751–1756.
- Casuso LA, Scott IU, Flynn HW, et al. Long-term follow-up of unoperated macular holes. *Ophthalmology*. 2001;108:1150–1155.
- Kim JW, Freeman WR, El-Haig W, Maguire AM, Arevalo JF, Azen SP. Baseline characteristics, natural history, and risk factors to progression in eyes with stage 2 macular holes. Results from a prospective randomized clinical trial. Vitrectomy for Macular Hole Study Group. *Ophthalmology*. 1995;102:1818–1829.
- Liang X, Liu W, Ohira A. Characteristics and risk factors for spontaneous closure of idiopathic full-thickness macular hole. *J Ophthalmol*. 2019;2019:4793764.